

## Sensing properties of optical fiber sensor to ultrasonic guided waves

Wensong Zhou<sup>\*1,2</sup>, Hui Li<sup>1,2a</sup>, Yongkang Dong<sup>3b</sup> and Anbang Wang<sup>1,2c</sup>

<sup>1</sup>Key Lab of Structures Dynamic Behavior and Control of the Ministry of Education, Harbin Institute of Technology, 73 Huanghe Road, Harbin 150090, China

<sup>2</sup>School of Civil Engineering, Harbin Institute of Technology, 73 Huanghe Road, Harbin 150090, China

<sup>3</sup>National Key Laboratory of Science and Technology on Tunable Laser, Harbin Institute of Technology, 2 Yikuang Street, Harbin 150001, China

(Received May 30, 2015, Revised August 8, 2015, Accepted August 20, 2015)

**Abstract.** Optical fiber sensors have been proven that they have the potential to detect high-frequency ultrasonic signals, in structural health monitoring field which generally refers to acoustic emission signals from active structural damages and guided waves excited by ultrasonic actuators and propagating in waveguide. In this work, the sensing properties of optical fiber sensors based on Mach-Zehnder interferometer were investigated in the metal plate. Analytical formulas were conducted first to explore the parameters affecting its sensing performances. Due to the simple and definable frequency component, the Lamb wave excited by the piezoelectric wafer was employed to study the sensitivity of the proposed optical fiber sensors with respect to the frequency, rather than the acoustic emission signals. In the experiments, according to above investigations, spiral shape optical fiber sensors with different size were selected to increase their sensitivity. Lamb waves were excited by a circular piezoelectric wafer, while another piezoelectric wafer was used to compare their voltage responses. Furthermore, by changing the excitation frequency, the tuning frequency characteristic of the proposed optical fiber sensor was also investigated experimentally.

**Keywords:** optical fiber sensor; guided wave; Mach-Zehnder interferometer; sensing property

### 1. Introduction

Acoustic emission and guided wave based methods are on the basis of elastic wave theory. These methods and techniques have been proven to be effective and promising tools for the local and small damage detection in structures, such as crack, corrosion, lamination *et al.* (Cawley and Alleyne 1996, Raghavan and Cesnik 2007, Carpinteri *et al.* 2007, Ma *et al.* 2015, Liu *et al.* 2016). In ultrasonic applications, the key essential procedure is the interaction between ultrasonic waves and the transducers, which are used to generate ultrasonic waves in structures are called actuators

---

\*Corresponding author, Associate Professor, E-mail: [zhouwensong@hit.edu.cn](mailto:zhouwensong@hit.edu.cn)

<sup>a</sup> Professor

<sup>b</sup> Professor

<sup>c</sup> Master Student

or transmitters, and used to capture ultrasonic waves are sensors or receivers. Actually, most of transducers can take as above both roles. The most common ultrasonic sensors include piezoelectric wafer (Sirohi and Chopra, 2000), magnetostrictive sensor (Kwun and Teller 1994), macro-fiber composite (Matt and Scalea 2007), EMAT sensor (Gao *et al.* 2010) and so on. The working mechanism of above sensors involves the transformation between mechanical energy and electric or magnetic energy, so they are affected more easily by electromagnetic interference. The other type of ultrasonic sensors is based on fiber-optic techniques. In comparison to the former, optical fiber sensors are immunity to electromagnetic interference. Moreover, they have very small dimensions and light weight and can be embedded unobtrusively within structures, have wide temperature operating range, and are capable to transmit signal over a long distance (Xiong and Cai 2012).

The type of optical fiber sensors can be differentiated according to the modulated physical parameters, such as by modulating the light phase, wavelength and so on. Early in 1977, Bucaro *et al.* (1977) of U.S. Naval Research Laboratory demonstrated the possibility of using an optical fiber to detect the ultrasonic signal by the phase modulation method. The acoustic field was produced by exciting a piezoelectric plate with the sinusoidal signal in a water filled tank, while the optical fiber coil was immersed in this acoustic field with various pressure and frequency. Experiments were carried out over the 40-400 kHz frequency range, and no significant change was found in sensitivity. In their investigation, the signal amplitude of ten turns fiber coil is ten times of the signal from a single turn. Gachagan *et al.* (1995) proposed a condition monitoring system that used a optical fiber as the sensors. Two groups of optical fibers were embedded across the composite plate, and a 633 nm Mach-Zehnder interferometer is used to demodulate acoustic signal, which was Lamb wave propagating in the plate. With this system, a delamination through the thickness of the composite plate was localized by analyzing reflection Lamb waves successfully in the laboratory. This experimental result can be considered as a fundamental basis for a structure health monitoring using the Mach-Zehnder interferometer-based optical fiber sensors. With the same interferometer, Pierce *et al.* (1996) compared the effectiveness of surface-bonded and embedded optical fibers for the detection of ultrasonic Lamb waves in steel, carbon fiber reinforced plastic and glass reinforced plastic plates. Experimental results indicated that the embedded optical fiber is about 20 times more sensitive to Lamb wave than the surface-bonded optical fiber, while the latter might be more practical due to the convenience. Gachagan *et al.* (1999) generated ultrasonic Lamb waves in thin composite plates by mean of a low profile acoustic source constructed using a flexible piezocomposite material, and detect the propagating waves by an optical fiber sensor, where light signal was demodulated by Mach-Zehnder interferometer. The optical fiber embedded in the plate or bonded on the surface of the plate kept straight shape in their experiments. Atherton *et al.* (2000) compared the ultrasonic signals detected by Mach-Zehnder and Michelson interferometers. The sensitivity of surface bonded and embedded fibers were also compared. All experimental results provided a greater insight into the detection mechanism and sensitivity of the Mach-Zehnder interferometer. Gong *et al.* (2001) proposed an amplitude-division-multiplexed interferometric sensor array for locating acoustic emission. Their experiments were conducted with a modified Mach-Zehnder interferometer consisting of two sensing arms and one reference arm.

Employing the other modulation techniques, the optical fiber can also detect the ultrasonic signals. Alcoz *et al.* (1990) presented a type of fiber-optic ultrasonic sensor, which consists of a continuous length of single mode optical fiber with Fabry-Perot interferometer built into it. In their experiments, the sensor was embedded in graphite-epoxy composite plate, in which the sinusoidal

acoustic field was generated by the piezoelectric disk, and the excitation frequency is in the range from 100 kHz to 5 MHz. Li *et al.* (2009) proposed an optical fiber sensor based on the Doppler effect of light wave transmission in optical fiber. The optical fiber sensors were designed as spiral, which resulted in the non-directionality sensitivity. Liang *et al.* (2013) proposed a type of Michelson interferometer with two optical fiber loop reflectors acoustic emission sensor to detect the vibrations produced by ultrasonic waves propagating in a solid body. Because of the decrease of the losses of light energy, the sensitivity of the system has been remarkably increased. Verstryngge *et al.* (2014) developed a polarization-modulated, single mode fiber optic sensor (FOS) and a global damage detection system. This system is applied successfully for the detection of acoustic emission in a full-scale concrete beam.

In this work, optical fiber sensors based on Mach-Zehnder interferometer will be investigated analytically and then experimentally. Aiming to develop more practical optical fiber sensor of ultrasonic waves, including acoustic emission signals and guided waves, for civil infrastructures, based on above investigations in literatures, this paper analyzed further the sensing properties of surface bonded optical fiber, used a spiral shape optical fiber sensor to receive the guided waves in the aluminum plate, i.e., Lamb waves, then compared the voltage response of the piezoelectric sensor and optical fiber sensor and analyzed the sensitivity to guided wave of different frequencies. Guided Lamb waves propagating in the thin plate are easy to be generated and their propagation paths and center frequencies can be defined distinctly. Therefore, they are employed to explore the sensing properties of optical fiber sensor in this work.

In the remaining part of this paper, the principle of Mach-Zehnder interferometer will be presented first. Then, the sensing properties of the optical fiber are analyzed. Lastly, guided wave generation and sensing using piezoelectric wafers and the proposed optical fiber sensor are investigated through experiments.

## 2. Mach-Zehnder interferometer and the optical fiber sensor

### 2.1 Mach-Zehnder interferometer

Mach-Zehnder interferometer is used to determine the relative phase shift variations between two light beams in two optical fibers, which are derived by splitting light from the same light source. The two optical fibers can be considered as sensing arm and reference arm respectively. As the indication by its name, the sensing arm is used to detect the acoustic field introduced by any mechanical behavior. The Mach-Zehnder interferometer is schematically presented in Fig. 1.

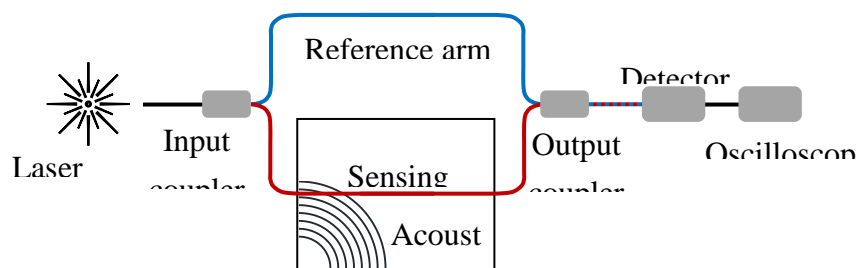


Fig. 1 Schematic of a Mach-Zehnder interferometer

The basis mechanism of Mach-Zehnder interferometer is the pressure induces the phase shift of the light beam. For these two arms, if the relative change in the phase of the light in sensing arm occurs with respect to the reference arm, the photodetector will output electrical signal, which is received by the oscilloscope. In ultrasonic applications, strain induced by guided waves or acoustic emission signals, which are elastic waves in nature, propagating in the structure will lead to the optical phase shift in sensing arm. In general, the relative phase change can be expressed as (Hocker 1979)

$$\Delta\phi = \beta\Delta L + L\Delta\beta = \beta\Delta L + L\frac{\partial\beta}{\partial n}\Delta n + L\frac{\partial\beta}{\partial D}\Delta D \quad (1)$$

where  $\beta$  is propagation constant of a single mode,  $\beta = k_0n$ .  $k_0$  is propagation constant of free-space propagation constant, and  $n$  is core index of the optical fiber.  $\beta\Delta L$  represents the effect of the physical change of length due to the strain.  $D$  is the diameter of the optical fiber. The third term in the above equation represents the change in the propagation constant owing to fiber diameter changing whose effect is negligible. Then Eq. (1) can be expressed as (Hocker 1979)

$$\Delta\phi \approx \beta L\varepsilon_{11} + Lk_0\Delta n \quad (2)$$

where  $\varepsilon_{11}$  is the strain in the direction of light propagation, i.e. the longitudinal direction of the optical fiber. The change in core index of optical fiber can be expressed as:

$$\Delta n = -\frac{n^3}{2}(p_{11}\varepsilon_{11} + p_{12}\varepsilon_{22} + p_{12}\varepsilon_{33}) \quad (3)$$

where  $p_{11}$ ,  $p_{12}$  and  $p_{13}$  the elements of the strain-optic tensor for a homogeneous isotropic material. Then, Eq. (1) can be expressed with three strain components

$$\Delta\phi \approx \beta L\varepsilon_{11} - \frac{1}{2}\beta Ln^2(p_{11}\varepsilon_{11} + p_{12}\varepsilon_{22} + p_{12}\varepsilon_{33}) \quad (4)$$

As can be seen, the phase change is proportional to the strain and length of the sensing arm, therefore, for the same strain, the larger  $L$ , the larger response of sensor.

## 2.2 Effects of the strain to the phase change

In this work, the proposed optical fiber ultrasonic sensor is used to detect ultrasonic Lamb waves in the plate, while in this case there are only three strain components:  $\varepsilon_{11}$ ,  $\varepsilon_{33}$  and  $\varepsilon_{13}$  (assume that 3 denotes thickness direction.), i.e., the state of plain strain. When the optical fiber is bonded on the surface of the plate by adhesive partially, according to above equations, shear strain  $\varepsilon_{13}$  can be ignored, so only  $\varepsilon_{11}$  and  $\varepsilon_{33}$  affect the relative phase change. Then sensitivities of the phase change to those strains are

$$\frac{\Delta\phi}{\varepsilon_{11}} \approx \beta L - \frac{1}{2}\beta Ln^2(p_{11} + 2\nu p_{12}) \quad (5)$$

$$\frac{\Delta\phi}{\varepsilon_{33}} \approx \nu\beta L - \frac{1}{2}\beta L n^2 (\nu p_{11} + \nu p_{12} + p_{12}) \quad (6)$$

where  $\nu$  is the Poisson's ratio.

All parameters representative of a He-Ne laser source and a fused silica optical fiber provided by Hocker (1979) are

$$\begin{aligned} n &= 1.456 & \beta &= 1.446 \times 10^7 \text{ m}^{-1} \\ p_{11} &= 0.121 & p_{12} &= 0.270 \\ \nu &= 0.17 \end{aligned} \quad (7)$$

Substitute above parameters to Eq. (6), for a one meter optical fiber, calculation indicates that the sensitivity of the phase change to strain  $\varepsilon_{11}$  is about four times larger than strain  $\varepsilon_{33}$ .

### 2.3 The spiral optical fiber ultrasonic sensor

Since the strain induced by guided waves is so small, which results in the insensitivity of the proposed sensors, in this work, the spiral optical fiber ultrasonic sensor is used to obtain as large as possible response of sensor, as shown in Fig. 2. For this spiral optical fiber sensor, it senses the area covered by the spiral, but not a point, so the signal received by the oscilloscope is related to the integral of strain along single direction in the area. Each turn of the spiral can be considered as a single circle, since the diameter of optical fiber is very small in comparison with the diameter of the spiral. For a single fiber circle, assume that it is bonded on the surface of a plate, where there is uniform strain field  $\varepsilon_{11}$ , the total deformation  $\Delta L_r$  can be expressed as

$$\Delta L_r = \int_0^{2\pi} \varepsilon_\theta r d\theta = \int_0^{2\pi} \varepsilon_{11} \cos^2 \theta r d\theta = \pi r \varepsilon_{11} \quad (8)$$

where  $r$  is the radius of the optical fiber circle.

For the second term in Eq. (2), the total change in core index of the circular optical fiber can be considered as the integral of the change in fiber of length  $rd\theta$ , so we have

$$L_r k_0 \Delta n_r = -\frac{1}{2} \beta \pi r n^2 (p_{11} \varepsilon_{11} + 2\nu p_{12} \varepsilon_{11}) \quad (9)$$

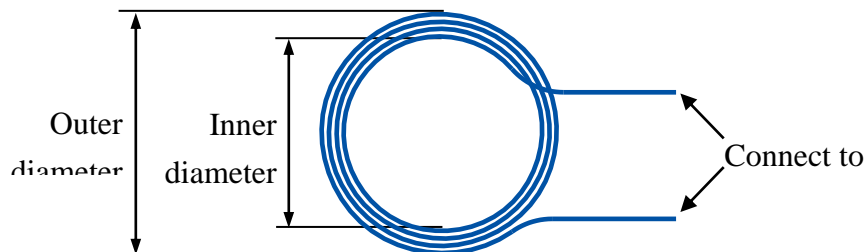


Fig. 2 The spiral optical fiber ultrasonic sensor

Thus, the phase change for a single circle optical fiber with radius  $r$  is

$$\Delta\phi_r \approx \beta\pi r \varepsilon_{11} - \frac{1}{2} \beta\pi r^2 (p_{11}\varepsilon_{11} + 2\nu p_{12}\varepsilon_{11}) \quad (10)$$

Eq. (9) indicates that the phase change for a circle optical fiber of length  $2\pi r$  is half of a straight optical fiber with the same length.

Finally, the total phase change for the spiral optical fiber is

$$\Delta\phi = \sum_{i=1}^n \Delta\phi_{r_i} \quad (11)$$

In addition, for the spiral sensor, small inner diameter leads to large optical power loss, so a minimum inner diameter needs to be determined experimentally. In practical applications, the outer diameter, inner diameter and number of turns may be changed to obtain different sensitivity.

Moreover, as we know, the conventional optical fiber sensor only measures the strain along its longitudinal direction, so it will be insensitive to the strain along the other directions, whereas the spiral optical fiber sensor has the same sensitivity to omni-direction.

### 3. Experimental investigation

The sensitivity of the optical sensor with respect to varying frequency signals is one of the most important properties. It relates to the sensor's operating frequency range determining which frequency range of acoustic emission or guided waves can be detected by the optical sensor. However, the sensitivity of the spiral optical fiber with respect to frequency is complicated due to following factors:

1) The optical fiber is bonded generally on the surface of the structure with super glue, which transfers the structural deformation to the optical fiber. The axial and bending stiffness of the optical fiber is much smaller than the structure because of its very small diameter. Thus, the flexible optical fiber adhering fully the structure will respond to the structural deformation in time. Moreover, according to Eq. (4), the relative phase change depends on the structural deformation only. From this point of view, the optical fiber sensor should have the almost same sensitivity to acoustic emission or guided wave signals with low and high frequency.

2) The ultrasonic acoustic emission or guided wave signals contain various or special frequency components, which corresponds to different wavelengths. When the wavelength is smaller than the length of optical fiber and the sum of the positive and negative strains along the optical fiber is very small, the relative phase change will be small with respect to the signals with specific frequency.

3) The preponderant displacement components for  $A_0$  and  $S_0$  modes Lamb wave is  $w$  in  $z$  direction and  $u$  in  $x$  direction, respectively, while the optical fiber sensor is more sensitive to displacement component  $u$  in  $x$  direction. This factor also affects the sensitivity of the optical fiber to ultrasonic signals.

Based on above reasons, in this work an experiment was designed to investigate the sensing properties of the optical fiber sensor to the Lamb waves propagating on the plate.

### 3.1 Experimental setup

The guided waves were generated on a thin aluminum plate by a piezoelectric wafer. In the plate, it's actually Lamb waves with  $A_0$  and  $S_0$  modes. Fig. 3 shows the dispersion curve (group and phase velocities) for  $A_0$  and  $S_0$  mode of Lamb waves respectively. Table 1 lists the corresponding wavelength for specific frequencies, which can be compared with the outer diameters of the optical fiber sensor loops. Fig. 4 shows the wave structure (i.e., modeshape of guided wave) for specific frequencies and modes. Because the  $A_0$  and  $S_0$  modes propagate with their different group velocities respectively, thus the waves with higher velocity will reflect and overlap the waves with slower waves, which results in difficulty in amplitude analysis. In the experiment, a large plate (1200.0 mm  $\times$  2400.0 mm  $\times$  1.0 mm) is used to extend the paths of wave reflections to avoid above problem. For comparison, another circular piezoelectric sensor was used to receive the Lamb waves at the same distance. All sensors and actuator are mounted on the top surface of the aluminum plate. The diameter of the circular piezoelectric wafers is 5 mm, and five sets of inner and outer diameters are used for optical fiber sensors, as listed in Table 2, in which the optical power loss was measured easily by optical power and energy meter. Their layout and location are shown in Fig. 5, in which the plate and wafers are not actual size. The super glue was used to attach these wafers on the plate. The actuator was driven by a function generator (AFG3252C, Tektronix, Inc.), into which a five-peaked narrow band signal was preprogrammed. It's defined by

$$x(t) = P \left[ H(t) - H\left(t - \frac{5}{f_c}\right) \right] \left[ 1 - \cos\left(\frac{2\pi f_c t}{5}\right) \right] \sin(2\pi f_c t) \quad (12)$$

where constant  $P$  is signal intensity,  $H(t)$  is Heaviside step function,  $f_c$  is the center frequency. This signal may reduce the dispersive effect of Lamb waves. Fig. 6 shows the signal with 100 kHz center frequency. The Mach-Zehnder interferometer consists of one RIO ORION Laser Module and one Thorlabs FPD510 photodetector mainly. The signals induced from the sensor were collected directly by a digital oscilloscope (DPO 2024, Tektronix, Inc.). The center frequencies of excitation signal  $f_c$  is varied from 25 kHz to 300 kHz in increments of 25 kHz for all test cases.

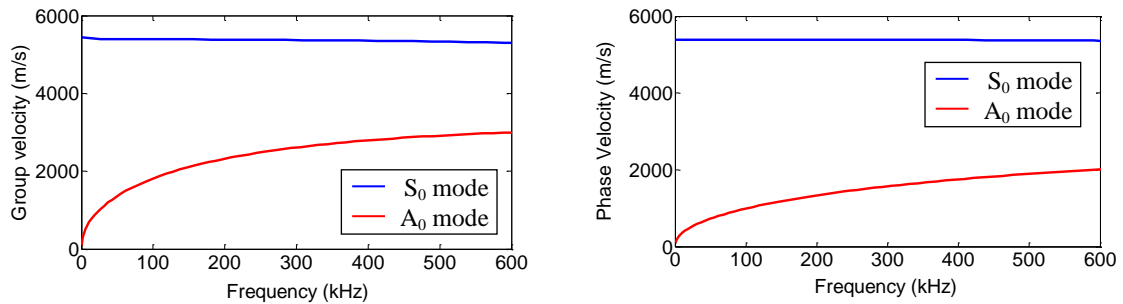


Fig. 3 Dispersion curves for Lamb waves

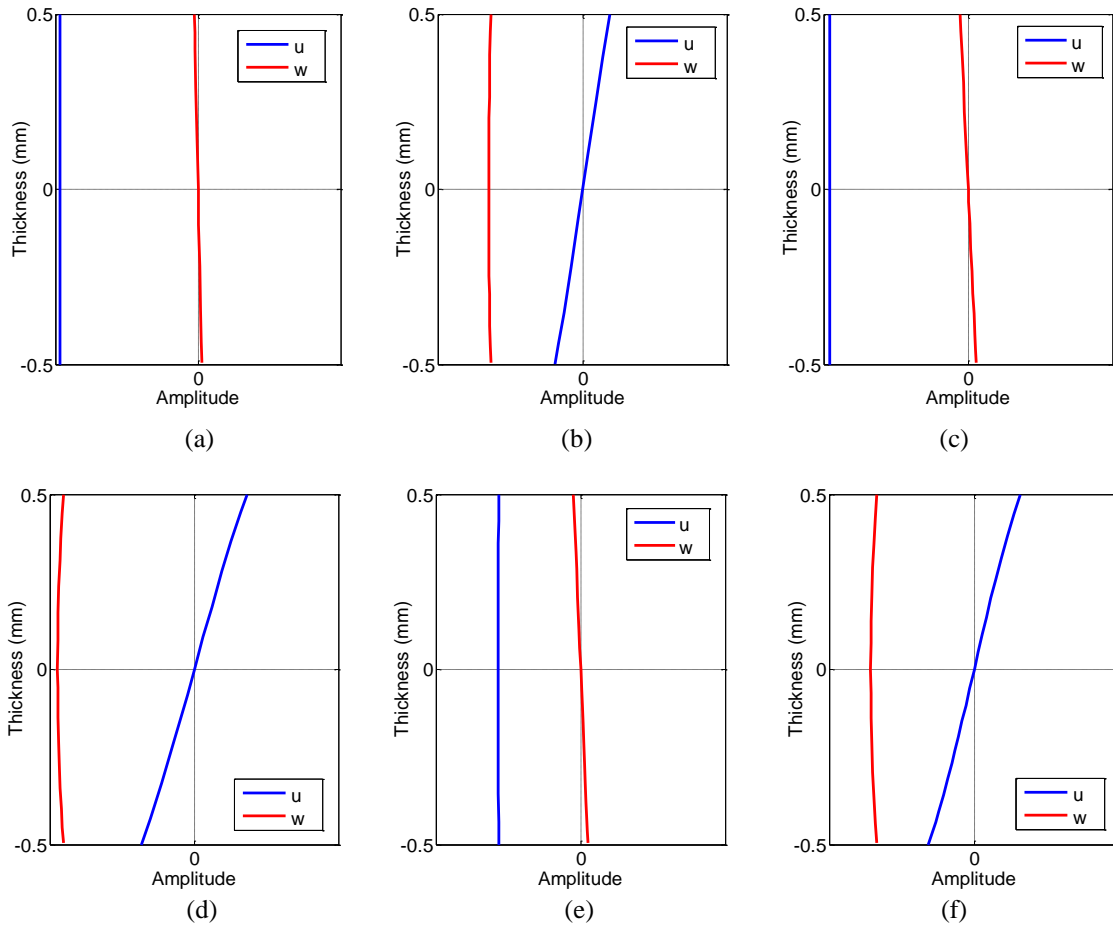


Fig. 4 Wave structure for Lamb waves: (a)  $f_c=100$  kHz,  $S_0$  mode, (b)  $f_c=100$  kHz,  $A_0$  mode, (c)  $f_c=200$  kHz,  $S_0$  mode, (d)  $f_c=200$  kHz,  $A_0$  mode, (e)  $f_c=300$  kHz,  $S_0$  mode and (f)  $f_c=300$  kHz,  $A_0$  mode

Table 1 Wavelength for Lamb waves in aluminum plate

Frequency (kHz)	$\lambda_S$ (mm)	$\lambda_A$ (mm)	Frequency (kHz)	$\lambda_S$ (mm)	$\lambda_A$ (mm)
25	215.8	19.6	175	30.8	7.0
50	107.9	13.7	200	27.0	6.5
75	71.9	11.1	225	24.0	6.1
100	53.9	9.5	250	21.6	5.7
125	43.1	8.5	275	19.6	5.4
150	35.9	7.7	300	18.0	5.2

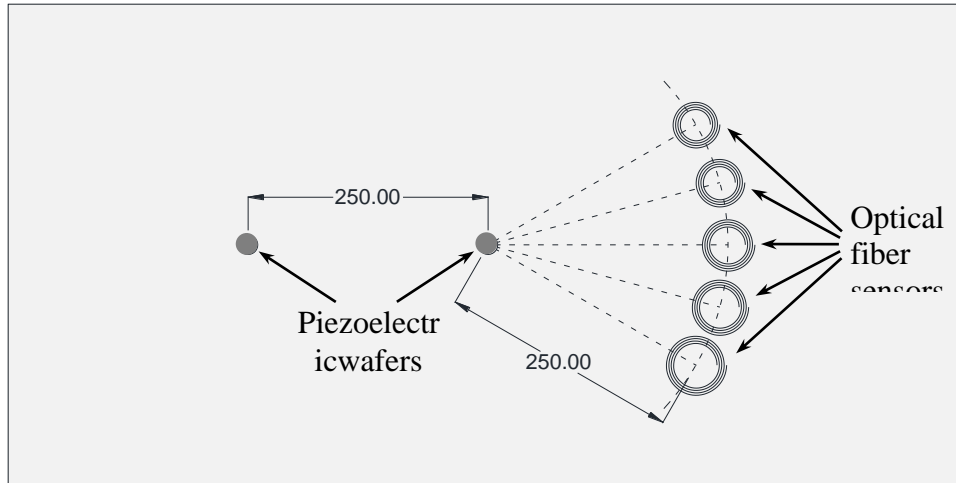


Fig. 5 Layout and location of sensors and actuator (unit: mm)

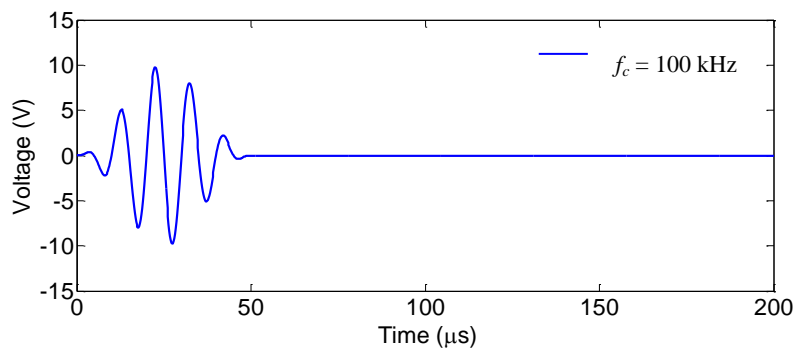


Fig. 6 Five-peaked narrow band excitation signal

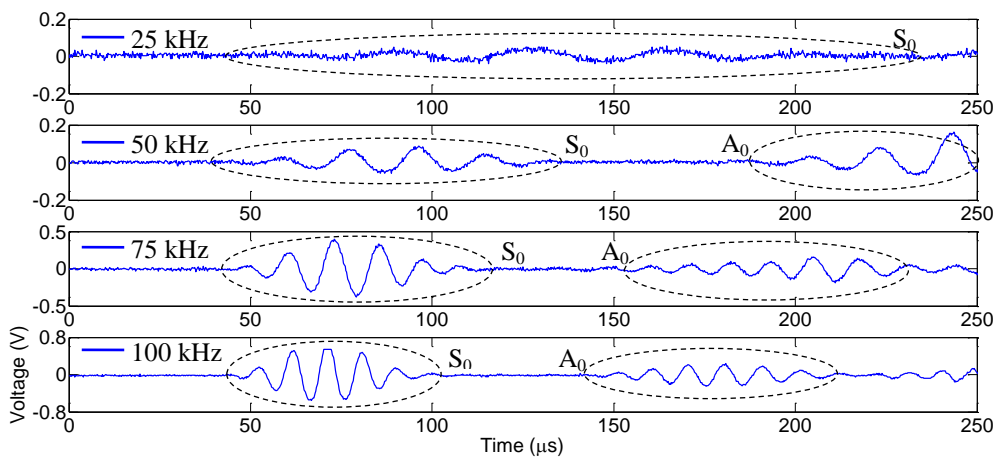
Table 2 Dimensions of the optical fiber sensor

Sensor No.	Inner diameter (mm)	Outer diameter (mm)	Power loss to (Input power: $970 \mu\text{w}$ )
1	15.0	25.0	$12 \mu\text{w}$
2	15.0	20.0	$36 \mu\text{w}$
3	17.0	25.0	$188 \mu\text{w}$
4	17.0	23.0	$201 \mu\text{w}$
5	20.0	30.0	$397 \mu\text{w}$

### 3.2 Results and analyses

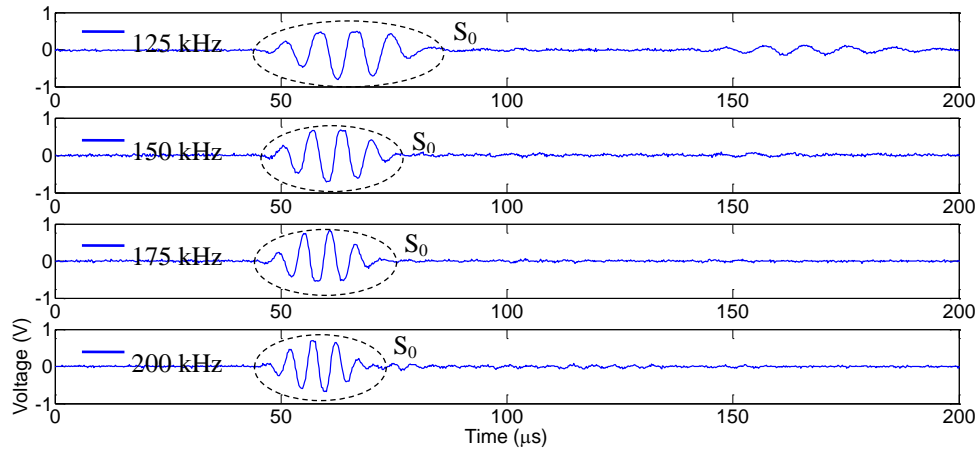
The pitch-catch method was used to detect Lamb waves propagating in the plate. At first, in the experiments, when the spiral inner diameters changed from 10 mm to 15 mm, the oscilloscope did not receive any signals. It indicates that for small inner diameters, the optical power loss is too much. When the inner diameters were increased to 15 mm, as listed in Table 2, obvious guided wave signals can be caught, but small inner diameters still lead to high optical power loss. In Table 2, sensor No. 5 with 20 mm inner diameter has the minimum optical power loss.

Fig. 7 shows all output voltage signals caught by the optical fiber sensor No. 5. According to time-of-arrival information, the wave modes can be recognized, as indicated in Fig. 7. In these figures, for all frequencies,  $S_0$  mode Lamb wave can be recognized from the voltage response curves according to their group velocities, while  $A_0$  mode of Lamb wave can be recognized just for low frequencies. Fig. 8 gives the voltage responses of the piezoelectric wafer for all frequencies. It can be found that the tuning frequency characteristic is similar to results for Lamb wave in thin-plate structure reported in literature (Giurgiutiu 2003). The difference is from the different geometry and physical parameters of wafer and plate. Fig. 9 shows the tuning frequency characteristic for the optical fiber sensor (No. 5) in this work, i.e., the sensitivity to different frequencies. Results for the other sensors are similar, so they are not shown here. The tuning characteristics indicated in this figure are different with those in Fig. 8. For the piezoelectric wafers, both actuator and sensor have their resonant frequencies, so the tuning frequency characteristics are affected by both actuator and sensor. This means that the strains themselves induced by the piezoelectric wafer change with the excitation frequencies. Therefore, if the strains can be measured and normalized, the sensitivity to different frequencies for the optical fiber sensor can be obtained. Actually, as a sensor, the optical fiber attached on the structure is capable to respond rapidly to the structural deformation in theory. The different sensitivity to guided wave with different frequency is induced by its dimension and the displacement characteristic of the specific wave mode.

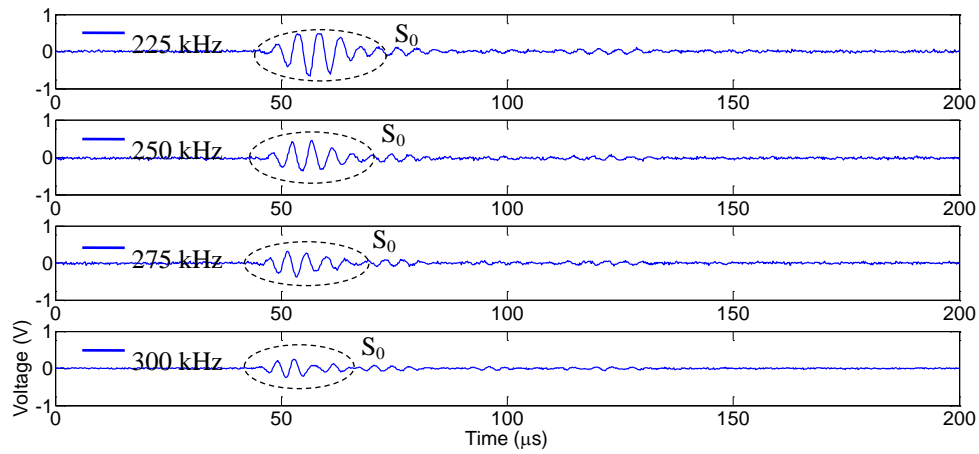


(a)

Continued-



(b)



(c)

Fig. 7 Experimental output voltage signals for different center frequencies: (a) 25 – 100 kHz, (b) 125 – 200 kHz and (c) 225 – 300 kHz

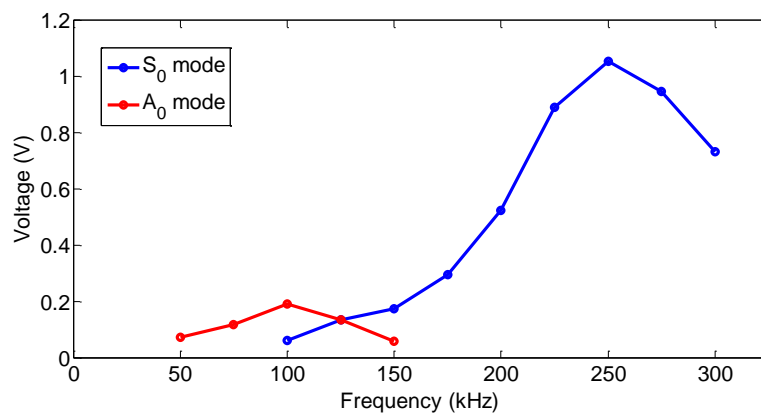


Fig. 8 Dependence of wave amplitude upon frequencies for the piezoelectric wafer

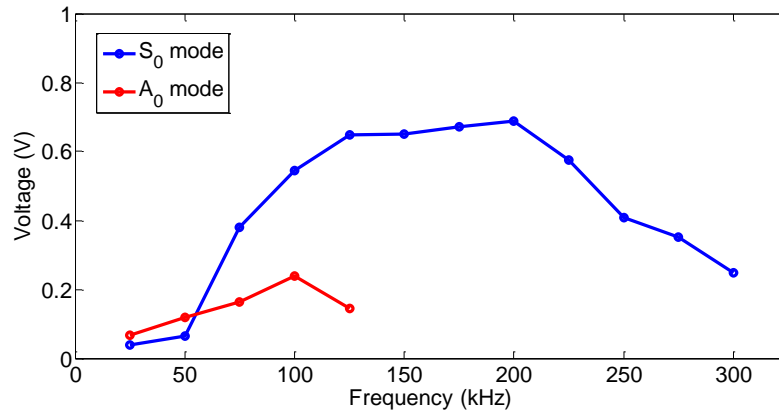


Fig. 9 Dependence of wave amplitude upon frequencies for the optical fiber sensors

In the experiment, the main displacement component for  $S_0$  mode is  $u$  in  $x$  direction, while  $A_0$  is in  $z$  direction (see Fig. 4). This results in the optical fiber sensor is insensitive to  $A_0$  mode, therefore the responding voltage outputs are very small in Fig. 7.

In addition, the dimension of the optical fiber sensor in this work is up to 25 mm, which is similar to the wavelength of Lamb wave below about 225 kHz for  $S_0$  mode and 20 kHz for  $A_0$  mode (see Table 1). For Lamb waves with small wavelength, the response of sensor is related to an average value of strain in the area covered by the sensor. Therefore, the sensor will be insensitive to Lamb wave with high frequency, and the wave shape becomes distortion slightly.

#### 4. Conclusions

The ultrasonic sensing properties of optical fiber sensors based on Mach-Zehnder are investigated in this work. Related results will be used to guide their practical applications, such as acoustic emission detection, guided waves based damage detection etc. According to the theoretical analysis, longer optical fiber may obtain higher change in phase, so the sensor is designed to the spiral form. In the experiments, both the piezoelectric wafers and the optical fiber sensors are bonded on the surface of an aluminum plate. The Lamb wave is excited by one of the piezoelectric wafer, while another piezoelectric wafer and the optical fiber sensors are used to receive the Lamb wave. Results from the experiments indicate that the optical fiber sensor with small diameter has very small response or is unable to receive the Lamb wave, because of the large optical power loss. The sensor response is also insensitive to the Lamb wave with small wavelength. Moreover, due to the predominant  $z$  direction displacement component of  $A_0$  mode, the sensor also has small output to this mode. It can be also deduced that for a pipe the optical fiber sensor is more sensitive to the modes, which has larger radial displacement component, such as  $L(0,1)$  etc. if the sensor winds round the circumference.

## Acknowledgments

The financial support from the National Key Technology R&D Program under Grant No. 2014BAG05B07, and the National Science Foundation of China under Grant No.50908066 are gratefully appreciated.

## References

- Alcoz, J.J., Lee, C.E. and Taylor, H.F. (1990), "Embedded fiber-optic fabry-perot ultrasound sensor", *IEEE T. Ultrason. Ferr.*, **37**(4), 302-306.
- Atherton, K., Dong, F., Pierce, G. and Culshaw, B. (2000), "Mach-Zehnder optical fiber interferometers for the detection of ultrasound", *Proceedings of SPIE*, **3986**, 27-34.
- Bucaro, J.A., Dardy, H.D. and Carome, E.F. (1977), "Optical fiber acoustic sensor", *Appl. Optics*, **16**(7), 1761-1762.
- Carpinteri, A., Lacidogna, G. and Pugno, N. (2007), "Structural damage diagnosis and life-time assessment by acoustic emission monitoring", *Eng. Fract. Mech.*, **74**, 273-289.
- Cawley, P. and Alleyne, D. (1996), "The use of Lamb waves for the long range inspection of large structures", *Ultrasonics*, **34**, 287-290.
- Gachagan, A., Hayward, G., McNab, A. and Reynolds, P. (1999) "Generation and reception of ultrasonic guided waves in composite plates using conformable piezoelectric transmitters and optical-fiber detectors", *IEEE T. Ultrason. Ferr.*, **46**(1), 72-81.
- Gachagan, A., Pierce, S.G., Philp, W.R., McNab, A., Hayward, G. and Culshaw, B. (1995), "Detection of ultrasonic Lamb waves in composite plates using optical-fibers", *IEEE Ultrasoncis Symp.*, 803-806.
- Gao, H., Ali, S. and Lopez, B. (2010), "Efficient detection of delamination in multilayered structures using ultrasonic guided wave EMATs", *NDT&E Int.*, **43**, 316-322.
- Giurgiutiu, V. (2003), "Lamb wave generation with piezoelectric wafer active sensors for structural health monitoring". *Proceeding of SPIE, Smart Structures And Materials*, **5056**.
- Gong, J., MacAlpine, J.M.K., Jin, W. and Liao Y. (2001), "Locating acoustic emission with an amplitude-multiplexed acoustic sensor array based on a modified Mach-Zehnder interferometer", *Appl. Optics*, **40**(34), 6199-6202.
- Hocker, G.B. (1979), "Fiber-optic sensing of pressure and temperature", *Appl. Optics*, **18**(9), 1445-1448.
- Kwun, H. and Teller, C.M. (1994), "Magnetostrictive generation and detection of longitudinal, torsional, and flexural waves in a steel rod", *J. Acoust. Soc. Am.*, **96**, 1202-1204.
- Li, F., Murayama, H., Kageyama, K. and Shirai, T. (2009), "Doppler effect-based fiber-optic sensor and its application in ultrasonic detection", *Opt. Fiber Technol.*, **15**, 296-303.
- Liang, Y., Qu, D. and Deng, Hu. (2013), "Based on optical fiber Michelson interferometer for acoustic emission detection experimental research", *Proc. of SPIE*, **8914**, 89140Z1-8.
- Liu, K., Wu, Z., Jiang Y., Wang Y., Zhou K. and Chen Y. (2016), "Guided waves based diagnostic imaging of circumferential cracks in small-diameter pipe", *Ultrasonics*, **65**, 34-42.
- Ma, S., Wu, Z., Wang Y. and Liu K. (2015), "The reflection of guided waves from simple dents in pipes", *Ultrasonics*, **57**, 190-197.
- Matt, H.M. and Scalea, F.L. (2007), "Macro-Fiber Composite piezoelectric rosettes for acoustic source location in complex structures", *Smart Mater. Struct.*, **16**, 1489-1499.
- Pierce, S.G., Philp, W.R., Gachagan, A., McNab, A., Hayward G. and Culshaw, B. (1996), "Surface-bonded and embedded optical fibers as ultrasonic sensors", *Appl. Optics*, **35**(25), 5191-5197.
- Raghavan, A. and Cesnik, C.E.S. (2007), "Review of guided-wave structural health monitoring", *Shock Vib. Dig.*, **39**, 91-114.
- Sirohi, J. and Chopra, I. (2000), "Fundamental understanding of piezoelectric strain sensors", *J. Intel. Mat. Syst. Str.*, **11**, 246-257.

- Verstrynge, E., Pfeiffer, H. and Wevers, M. (2014), "A novel technique for acoustic emission monitoring in civil structures with global fiber optic sensors", *Smart Mater. Struct.*, **23**, 065022.
- Xiong, W. and Cai, C.S. (2012), "Development of fiber optic acoustic emission sensors for applications in civil infrastructures", *Adv. Struct. Eng.*, **15**(8), 1471-1486.